



1-2009

Differentiation and Regenerative Capacities of Human Odontoma-Derived Mesenchymal Cells

Jin-Seon Song
University of Pennsylvania

Derek Stefanik
University of Pennsylvania

Monika Damek-Poprawa
University of Pennsylvania

Faizan Alawi
University of Pennsylvania

Sunday O. Akintoye
University of Pennsylvania

Follow this and additional works at: https://repository.upenn.edu/dental_papers

 Part of the [Dentistry Commons](#)

Recommended Citation

Song, J., Stefanik, D., Damek-Poprawa, M., Alawi, F., & Akintoye, S. O. (2009). Differentiation and Regenerative Capacities of Human Odontoma-Derived Mesenchymal Cells. *Differentiation*, 77 (1), 29-37. <http://dx.doi.org/10.1016/j.diff.2008.09.005>

This paper is posted at ScholarlyCommons. https://repository.upenn.edu/dental_papers/136
For more information, please contact repository@pobox.upenn.edu.

Differentiation and Regenerative Capacities of Human Odontoma-Derived Mesenchymal Cells

Abstract

Regenerating human tooth *ex vivo* and biological repair of dental caries are hampered by non-viable odontogenic stem cells that can regenerate different tooth components. Odontoma is a developmental dental anomaly that may contain putative post-natal stem cells with the ability to differentiate and regenerate *in vivo* new dental structures that may include enamel, dentin, cementum and pulp tissues. We evaluated odontoma tissues from 14 patients and further isolated and characterized human odontoma-derived mesenchymal cells (HODCs) with neural stem cell and hard tissue regenerative properties from a group of complex odontoma from 1 of 14 patients. Complex odontoma was more common (9 of 14) than compound type and females (9 of 14) were more affected than males in our set of patients. HODCs were highly proliferative like dental pulp stem cells (DPSCs) but demonstrated stronger neural immunophenotype than both DPSCs and mandible bone marrow stromal cells (BMSCs) by expressing higher levels of nestin, Sox 2 and β III-tubulin. When transplanted with hydroxyapatite/tricalcium phosphate into immunocompromised mice, HODCs differentiated and regenerated calcified hard tissues *in vivo* that were morphologically and quantitatively comparable to those generated by DPSCs and BMSCs. When transplanted with polycaprolactone (biodegradable carrier), HODCs differentiated to form new predentin on the surface of a dentin platform. Newly formed predentin contained numerous distinct dentinal tubules and an apparent dentin-pulp arrangement. HODCs represent unique odontogenic progenitors that readily commit to formation of dental hard tissues.

Keywords

Odontoma, Dentin, Tooth regeneration, Odontoblasts, Mesenchymal

Disciplines

Dentistry



Published in final edited form as:

Differentiation. 2009 January ; 77(1): 29–37. doi:10.1016/j.diff.2008.09.005.

Differentiation and Regenerative Capacities of Human Odontoma-Derived Mesenchymal Cells

Jin-Seon Song¹, Derek Stefanik², Monika Damek-Poprawa², Faizan Alawi³, and Sunday O. Akintoye^{2,*}

¹Department of Endodontics, University of Pennsylvania, Philadelphia PA

²Department of Oral Medicine, University of Pennsylvania, Philadelphia PA

³Department of Pathology, School of Dental Medicine, University of Pennsylvania, Philadelphia PA

Abstract

Regenerating human tooth *ex vivo* and biological repair of dental caries are hampered by non-viable odontogenic stem cells that can regenerate different tooth components. Odontoma is a developmental dental anomaly that may contain putative post-natal stem cells with the ability to differentiate and regenerate *in vivo* new dental structures that may include enamel, dentin, cementum and pulp tissues. We evaluated odontoma tissues from 14 patients and further isolated and characterized human odontoma-derived mesenchymal cells (HODCs) with neural stem cell and hard tissue regenerative properties from a group of complex odontoma from 1 of 14 patients. Complex odontoma was more common (9 of 14) than compound type and females (9 of 14) were more affected than males in our set of patients. HODCs were highly proliferative like dental pulp stem cells (DPSCs) but demonstrated stronger neural immunophenotype than both DPSCs and mandible bone marrow stromal cells (BMSCs) by expressing higher levels of nestin, Sox 2 and β III-tubulin. When transplanted with hydroxyapatite/tricalcium phosphate into immunocompromised mice, HODCs differentiated and regenerated calcified hard tissues *in vivo* that were morphologically and quantitatively comparable to those generated by DPSCs and BMSCs. When transplanted with polycaprolactone (biodegradable carrier), HODCs differentiated to form new predentin on the surface of a dentin platform. Newly formed predentin contained numerous distinct dentinal tubules and an apparent dentin-pulp arrangement. HODCs represent unique odontogenic progenitors that readily commit to formation of dental hard tissues.

Keywords

Odontoma; Dentin; Tooth regeneration; Odontoblasts; Mesenchymal

Introduction

Post-natal stem cells have been isolated from different dental tissues including dental pulp (Gronthos et al., 2000), periodontal ligament (Seo et al., 2004), Hertwig's root sheath (Sonoyama et al., 2007), exfoliated deciduous teeth (Miura et al., 2003) and cementum (Grzesik et al., 1998). Each of these only regenerated one of the different tooth components that include enamel, dentin, cementum, periodontal ligament and dental pulp. Identifying dental stem cells capable of regenerating majority, if not all the tooth components are still ongoing. Odontoma,

*To whom all correspondence should be addressed. **Corresponding Author:** Sunday O. Akintoye BDS, DDS, MS, University of Pennsylvania, School of Dental Medicine, Department of Oral Medicine, The Robert Schattner Center Room 209, 240 South 40th Street, Philadelphia PA 19104, Phone: 215-898-9932, Fax: 215-573-7853, akintoye@dental.upenn.edu.

a developmental malformation composed of disorganized normal dental tissues may contain stem cell populations with unique ability to regenerate different tooth components. An odontoma that contains multiple well-formed miniature teeth is referred to as a compound odontoma while one with heterogeneous mixture of irregular tooth-like structures such as enamel, dentin, cementum, pulp tissue and odontogenic epithelium is referred to as a complex odontoma (Sapp et al., 2004). Within an odontoma, is a rich network of undifferentiated cells that have not been clearly defined. The ability of these cells to form complex tooth structures and direct spatial relationships of enamel, dentin and cementum is still unclear. Despite association of odontomas with various developmental disorders of neuroectodermal origin (el-Saggan et al., 1998), odontomas are generally regarded as hamartomas (abnormal mixture of normal tissue elements) and not neoplastic proliferations (Sapp et al., 2004). Although dental lamina that initiates tooth development is formed from epithelial-mesenchymal interactions (Thesleff et al., 1991; Thesleff and Hurmerinta, 1981), the human odontogenic ectomesenchyme is derived from neural crest (Sharpe, 2001; Slavkin et al., 1988). Cell-fate determination and neural crest induction are also mediated by Wnt protein (Garcia-Castro et al., 2002). Specifically, Wnt/ β -catenin signaling initiates 'de novo' formation of teeth (Thesleff et al., 1995; Yamashiro et al., 2007). Several neural crest-derived tissues like dental pulp, periodontal ligament and maxilla/mandible have unique site-specific post-natal stem cells (Gronthos et al., 2000; Seo et al., 2004; Akintoye et al., 2006). So it is possible that odontoma originating from neural crest also contain multipotent post-natal stem cells that can be induced *in vitro* to differentiate into dental tissues.

Putative post-natal stem cells isolated from adult and deciduous teeth have limited regenerative capacity and form hard tissues that are still far from an anatomically or histologically precise tooth structure (Gronthos et al., 2000). Stem cells derived from the apical dental papilla exhibited greater capacity for dentin regeneration than those derived from dental pulp. Moreover, transplantation of a composite of apical papilla stem cells with periodontal ligament stem cells regenerated *in vivo* a well-formed root complex that was able to support a fixed porcelain crown (Sonoyama et al., 2006). While these results are promising, regenerating all the tooth components will require recapitulation of the embryonic tooth environment using highly pluripotent stem cells. Odontomas may be a viable source of multipotent odontogenic stem cells that readily differentiate into dental tissues. It is therefore conceivable that human odontoma contains post-natal stem cells that readily commit to dental differentiation and apparently able to form majority of the dental tissues including enamel, dentin, cementum and pulp.

This study tested the hypothesis that a niche of neural crest-associated post-natal stem cells with dental regenerative capacity reside in odontomas. We identified highly proliferative human odontoma-derived mesenchymal cells (HODCs) that shared stem cell characteristics with dental pulp stem cells (DPSCs) and bone marrow stromal cells (BMSCs). When transplanted into immunocompromised mice, HODCs regenerated highly differentiated dentin, cementum and pulp-like tissues *in vivo*, making them a unique population of odontogenic progenitor cells.

Methods

Patients and tissue sampling

Fourteen patients with radiographically-diagnosed odontoma were enrolled in a tissue-collection clinical protocol (#417200) approved by the University of Pennsylvania after written informed consent. Cells were harvested from one 7 year-old female patient with a group of complex odontomas in the right maxilla (Figure 1). Half of the odontoma samples were fixed in 4% PFA for histological analysis while the other half were immediately placed in cold α -MEM for cell culture and further analysis.

Cell culture

Isolation of human odontoma-derived cells (HODCs) was done using an established protocol for isolation of human trabecular bone cells (Robey, 1995) described briefly. The pieces of odontoma tissues were carefully cleaned with sterile surgical blade to remove any contaminating soft tissues. The samples were broken into smaller fragments with sharp surgical scissors in a reaction vial containing enzyme medium made of Dulbecco's modified Eagle's medium (DMEM; plus high glucose and glutamine) and Ham's F-12 medium (Invitrogen, Life Technologies, Carlsbad, CA) at 1:1 ratio, 100 IU/ml penicillin, 67 mmol/l streptomycin sulfate, 0.13 mmol/l sodium L-ascorbate and 1 mmol/l calcium. Repeated fragmentation in several changes of enzyme medium was carried out until samples became granular. The odontoma granules were digested with 250 IU/ml Collagenase P (Cat # 11213873001, Roche Applied Science, Indianapolis, IN) in enzyme medium for 2 hours at 37 °C. After repeated washes in enzyme medium, the odontoma granules were seeded in 150 mm culture dish containing growth medium made of DMEM and Ham's F-12 medium (1:1), 100 IU/ml penicillin, 67 mmol/l streptomycin sulfate, 0.13 mmol/l sodium L-ascorbate and 10% fetal bovine serum (Equitech Bio Inc, Kerville, TX) incubated at 37 °C in a humidified atmosphere of 6% CO₂ and air. Medium was changed twice per week and human odontoma-derived cells (HODCs) that emerged from the odontoma granules were maintained in culture until 75% confluence. Sub-confluent primary HODCs were released with trypsin-EDTA (Invitrogen, Life Technologies, Carlsbad, CA) and stored in liquid nitrogen until tested. Control postnatal stem cells compared with HODCs were dental pulp stem cells (DPSCs) and mandible bone marrow stromal cells (BMSCs) from gender-matched 20 year-old normal volunteer enrolled in an institutionally-approved protocol at the University of Pennsylvania (protocol # 709137). These were isolated and cultured as previously described (Akintoye et al., 2006; Gronthos et al., 2000). Primary culture of DPSCs and BMSCs were established in α -Minimum Essential Medium (α -MEM) supplemented with 100 IU/ml penicillin, 67 mmol/l streptomycin sulfate, 0.13 mmol/l sodium L-ascorbate and 10% fetal bovine serum. For all experiments, HODCs were compared in parallel with DPSCs and BMSCs. Early passage (passage 2 or 3) cells were tested.

Cell proliferation assay

HODCs, DPSCs and BMSCs were seeded at 1×10^4 cells/cm² in triplicate wells of 96-well plates. Proliferative capacity of HODCs was assessed in two phases (early, within 96 hours and late, within 12 days) using the colorimetric WST-1 assay (Cat #11644807001, Roche Applied Science, Indianapolis IN), as previously described (Stefanik et al., 2008). Absorbance (A₄₅₀) was measured against a background control using a Multiskan MCC microplate photometer (Thermo Fisher Scientific, Waltham, MA).

Telomerase activity

The expression of telomerase in enzymatically active sub-confluent second passage cells was measured by telomeric repeat amplification protocol using the TRAPEZE Telomerase Detection Kit (Catalogue #S7700, Chemicon International, Temecula, CA), according to the manufacturer's protocol as previously described (Akintoye et al., 2006). Briefly, the cells were released with trypsin-EDTA, washed with PBS and lysed with CHAPS buffer provided with the kit. Protein concentration of the samples was determined using BCA Protein Assay Kit (Catalogue #23227, Pierce, Rockford, IL). 1.5 μ g of cell extract was used for each PCR reaction in a Perkin Elmer thermocycler (Perkin Elmer, Boston, MA). Samples were pre-incubated at 30°C for 30 minutes before the 2-step PCR at 94°C/30s and 59°C/30s for 40 cycles. HeLa cell extract and telomerase quantitation control template (TSR8) served as positive controls. Negative controls included heat-treated samples and primer-dimer/PCR contamination control. 25 μ l of the PCR products were separated on a 10% TBE gel (Catalogue #EC6275, Invitrogen,

Carlsbad, CA) under non-denaturing conditions and the bands were visualized by staining with ethidium bromide.

Immunocytochemistry

The three cell types were seeded at 8000 cells/well in 8-well chamber slides (Nalge Nunc, Rochester, NY) and cultured until cells were 60–70% confluent. Subsequently, the cells were washed with PBS (pH 7.4) and fixed with 4% paraformaldehyde in PBS. A set of cells was stained using Human Neural Stem Cell Characterization Kit (Catalogue #SCR060, Chemicon International, Temecula, CA) according to manufacturer's recommendation with the following modifications. After blocking with 1% BSA in PBS for 2 hours at room temperature, cells were incubated overnight at 4 °C with the following primary antibodies: 1:100 dilution of mouse anti-nestin and 1:100 dilution of rabbit anti-Sox 2. After washing, the samples were incubated for 1 hour at room temperature with 1:400 dilution of fluorescent-labeled specie-specific secondary antibodies that included goat anti-mouse Alexa Fluor 488 and goat anti-rabbit Alexa Fluor 555 (Invitrogen, Carlsbad, CA). Nuclei were visualized with 2.8 µmol/l of DAPI. Negative controls were incubated with non-immune rabbit serum and purified mouse IgG control antibody provided with the kit. Additional sets of cells were stained using mouse monoclonal antibody to dentin matrix protein 1 (LFMb-31; anti-DMP1) (Ogbureke and Fisher, 2004) (gift from Dr. L.W. Fisher, National Institute of Dental and Craniofacial Research/ National Institutes of Health (NIDCR/NIH), Bethesda, MD). Specimens were serially excited and images were captured on a Bio-Rad Radiance 2100 scanning laser confocal microscope (Bio-Rad Laboratories, Hercules, CA), using the same laser settings.

Phenotype of single colony-derived strains of HODCS

Primary HODCs were re-plated in 150 mm dishes at 1.0×10^3 cells/ml to establish single colony-derived stains of HODCs (passage 2). The colonies that formed from individual cells were monitored microscopically for 14 days to avoid adjacent clones merging together. Absolutely round colonies with more than 50 cells per colony were selected for further expansion using a modification of a previously described method (Kuznetsov et al., 1997) Briefly, the cell monolayer was rinsed twice with PBS (pH 7.4). Polystyrene cloning cylinders (Sigma Aldrich, St Louis, MO) were attached to the culture dish with high vacuum grease (Dow Corning, Midland MI) so that majority of the cells constituting a clone were enclosed within the cylinder circumference. All 8 clones with ≥ 50 cells per clone were selected. The encircled cells within each cloning cylinder were released with trypsin-EDTA and transferred to separate wells of a 6-well plate for further expansion. Immunophenotype of 4 randomly selected clones (4 of 8 clones) was performed in 6-well chamber slides as described above.

Immunohistochemistry of odontoma tissues

Deparaffinized 5 µm sections of human odontoma tissue were immunostained using the following primary antibodies: mouse monoclonal antibody to dentin matrix protein 1 (LFMb-31; anti-DMP1) and dentin sialophosphoprotein (LFMb21, anti-DSPP) (gifts from Dr. L. W. Fisher, NIDCR/NIH, Bethesda, MD) (at 1: 100 dilution); mouse monoclonal anti-β-catenin (sc-59737) and goat polyclonal anti-Wnt-1 (sc-6280) (both from Santa Cruz Biotechnology Inc. Santa Cruz CA) (at 1:200 dilution). Reactivity of the antibodies was subsequently visualized with the DakoCytomation EnVision+ Dual Link system-HRP (DAB +) kit (Catalogue # K4065, Dako North America, Carpinteria, CA) following manufacturer's recommendations. Negative controls omitted primary antibodies substituted with non-immune serum for goat antibody and IgG isotype control for monoclonals.

Cell transplantation and assessment of *in vivo* cell differentiation

In vivo differentiation of HODCs was compared with DPSCs and BMSCs under University of Pennsylvania-approved animal protocol (#800209). For evaluation of *in vivo* differentiation, 2×10^6 cells attached to 40 mg of spheroidal hydroxyapatite/tricalcium phosphate (HA/TCP, particle size 0.5–1.0 mm, Zimmer, Warsaw, IN) were transplanted into separate subcutaneous pockets of 4 week-old immunocompromised nude female mice (NIH-III-nu, Charles River Laboratories, Wilmington, MA) as previously described (Akintoye et al., 2006). Transplants were placed in at least three animals per cell type. Transplants were harvested at 11 weeks, fixed in 4% paraformaldehyde in PBS (pH 7.4), decalcified in 10% EDTA in PBS (pH 8.0) and embedded in paraffin. 5 μ m sections were stained with hematoxylin/eosin (H&E) for histological evaluation. *In vivo* differentiation of HODCs into dental tissues was assessed by transplantation of HODCs within a shell of decalcified human dentin. Both DPSCs and BMSCs arising embryologically from neural crest were used as controls. DPSCs served as a positive control while BMSCs served as negative control for dental cells. Human dentin shell was prepared from roots of extracted teeth. Teeth were cleaned of all soft tissues, fixed with 4% paraformaldehyde (PFA) and decalcified with Immunocal® (Decal Chemical Corporation, Tallman, NY). A tungsten carbide #557 fissure bur attached to a slow speed dental hand-piece was used to remove residual pulp tissue and expand the root canal. Each tooth root was transformed to a soft dentin shell with a central canal and sectioned into 8 mm pieces. Each dentin shell was filled with a composite of 2×10^6 cells attached to 40 mg of polycaprolactone (PCL) granules (CAPA® 6506, particle size 0.6 mm, Solvay Caprolactones, Houston TX), a water-insoluble, biodegradable carrier. Negative controls consisted of tooth shells filled with PCL without cells. The dentin shells were transplanted in duplicates, subcutaneously into immunocompromised nude female mice as described above. Transplants were harvested at 6 weeks, fixed in 4% paraformaldehyde in PBS (pH 7.4), decalcified in 10% EDTA (pH 8.0) and embedded in paraffin. 5 μ m sections were stained with H&E as above for histological evaluation. The human origin of cells within transplants was confirmed by immunostaining with anti-human DMP1 and specificity of anti-human DMP1 was reconfirmed using mouse dentin as negative control.

RNA isolation and real-time PCR

Total RNA was isolated from cell monolayer using TRIzol® reagent (Invitrogen Life Technologies, Carlsbad, CA) following manufacturer's recommendations. cDNA was prepared from 2 μ g total RNA using oligo(dT) and the SuperScript First-Strand Synthesis System for RT-PCR (Invitrogen Life Technologies, Carlsbad, CA). Real time PCR analysis of HODCs, DPSCs and BMSCs was performed in a LightCycler 2.0 (Roche Applied Science, Indianapolis, IN) with LightCycler Fast-Start DNA Master SYBR Green I kit (Roche Applied Science) using primers specific for human alkaline phosphatase, GenBank Accession number NM000478, fragment size 161 bp, forward, 5'-ACCATTCCCACGTCTTCACATTTG-3'; reverse, 5'-AGACATTCTCTCGTTCACCGCC-3' and human nestin, GenBank Accession number NM006617, fragment size 717 bp, forward 5'-GGCAGCGTTGGAACAGAGGTTGGA-3' and reverse 5'-CTCTAAACTGGAGTGGTCAGGGCT-3'. Gene expression was normalized with human GAPDH, GenBank Accession number M33197, fragment size 816 bp, forward, 5'-AGCCGCATCTTCTTTTGCCTC-3'; reverse, 5'-TCATATTTGGCAGGTTTTTCT-3'. Real time RT-PCR data were obtained as crossing points converted to arbitrary units of mRNA assuming a concentration-dependent straight line for a semi-log plot as previously described (Osyczka et al., 2004). The slope (fold change in mRNA/cycle) was set at 3.5 with crossing point cycle number serving as an estimate of the y-intercept. A final melt curve from 60 – 95° C was performed to confirm specificity of the PCR reaction. The identities of PCR products were checked by gel electrophoresis.

Statistical analysis

HODCs were compared with DPSCs and BMSCs using one-way analysis of variance (ANOVA) followed by post hoc Holm-Sidak test. Differences were considered significant at $P < 0.05$.

Results

Isolation and characteristics of HODCs

There were more females (64%) in this cohort of odontoma patients. Histologically, the odontomas were identified as complex ($n = 9$) and compound ($n = 5$) types (Table 1). Most of the odontomas developed in the posterior jaw except two identified in the anterior jaw. A representative complex odontoma located in the right maxilla is shown impeding the eruption of right first permanent molar (Figure 1). Surgical removal of the odontomas was uneventful. Histological examination of the complex odontomas revealed irregular solitary masses composed of variable amounts of enamel, dentin, cementum and pulp tissue. A sample from another patient demonstrated previously described isolated areas of melanin pigmentation (data not shown) (Ernst et al., 2007). Histological analysis of odontoma presented in Figure 1 showed an outer dentin layer surrounding an inner enamel core, amorphous matrix and abundant heterogeneous fibroblast-like cells (Figure 2 A, B, C). In one complex odontoma, the cellular components that were used to isolate HODCs expressed Wnt-1 and β -catenin known to be associated with pre-migratory neural crest cells (Figure 2 D, E) but the outer dentin layer was negative. HODCs were also positive for nestin and Sox 2 (two early neural stem cell markers) and β III-tubulin (a late stem cell marker) (Figure 3 A, B, C), an indication of a heterogeneous population of neural crest-associated stem cells and neuronally-committed cells (Lendahl et al., 1990;Graham et al., 2003). Comparatively, both DPSCs and mandible BMSCs were positive for nestin (Figure 3 D, E) but negative for Sox 2 and β III-tubulin (data not shown). The level of nestin assessed by real-time PCR was much higher in HODCs ($P < 0.04$) than either DPSCs or BMSCs (Figure 3F) which is consistent with the high expression of nestin in neural progenitor cells, an indication of the multipotent property of HODCs. The HODCs single clones isolated were positive for nestin and Sox 2, two markers of early neural stem cell progenitors (Figure 4). Morphologically, the HODC single clones acquired stretched-out dendrite-like cytoplasmic projections like neural cells. Sox 2 did not appear to be co-localized with nestin in HODCs (Figure 4).

Survival capacity of HODCs

Proliferative and survival capacities of HODCs compared favorably well with both DPSCs and BMSCs, which are also neural crest-derived postnatal stem cells. HODCs proliferation was initially slow within the first 96 hours like mandible BMSCs (Figure 5A). However, proliferative capacity dramatically increased after 4 days to pattern that of DPSCs (Figure 5B) despite comparative presence of telomerase in the three cell types as demonstrated by the TRAPeze assay (Figure 5C). This suggests superior survival and rapid population doubling potential of HODCs compared to BMSCs. There was some heterogeneity in the proliferative capacity of the single colony-derived strains of HODC based on cell population. However, all the single clones were homogeneously immunoreactive to nestin (Figure 4).

In vitro and *in vivo* odontogenic differentiation capacity of HODCs

The enamel, dentin and cells within the odontoma (Figure 6 A, B, C) as well as HODCs (Figure 6D) expressed DMP1 just like DPSCs (Figure 6E). However, only the cellular contents in odontoma were positive for the odontoblast-specific marker, DSPP (Figure 6F) while both HODCs and DPSCs were negative. This suggests an undifferentiated HODC phenotype as previously described in DPSCs (Gronthos et al., 2000). When HODCs were attached to HA/

TCP and transplanted subcutaneously into immunocompromised mice, they regenerated hard tissue nodules with entrapped cells (Figure 7A). The nodules resembled that formed by similarly transplanted BMSCs which also contained abundant osteocyte-like cells but were slightly different from those formed by DPSCs which did not contain entrapped cells (Figure 7 B, C). HODCs attached to HA/TCP regenerated hard tissues that appeared structurally akin to bone or cellular cementum which are known to be histologically similar, but DPSCs formed hard tissues structurally resembling acellular cementum. Using an established semi-quantitative analysis, hard tissue formation was scored on a scale of 0 to 4 as follows: 0 (no hard tissue nodules evident within the transplant), 1 (minimal nodules evident [1 hard tissue nodule]), 2 (weak nodule formation occupying only a small portion of the transplant), 3 (moderate nodule formation occupying a significant portion but less than 50% of the transplant) and 4 (abundant hard tissue nodules, occupying more than 50% of the transplant ± hematopoietic cells) (Kuznetsov et al., 1997). This scoring system has been verified by histomorphometry and confirmed to be reliable (Mankani et al., 2001). It showed that HODCs and DPSCs induced more hard tissues quantitatively than BMSCs (Figure 7D) despite much lower levels of alkaline phosphatase expression by HODCs and DPSCs ($P < 0.001$) (Figure 7E). This could be a reflection of long-term proliferative capacity, possible delayed senescence and commitment to an odontogenic rather than an osteogenic lineage. It also highlights similarities between HODCs and DPSCs as well as their differences from BMSCs. Interestingly, when HA/TCP was replaced with PCL and the “cell-PCL” composite was transplanted within a defined dentin environment, only HODCs deposited a new layer of hard tissue that resembled dentin matrix or predentin (Figure 7 F, G, H). The space occupied by resorbed PCL was filled by abundant HODCs actively secreting predentin. These spaces remained unfilled in both DPSC and BMSC transplants. Immunostaining of the transplants with anti-human DMP1, which is human tissue specific, showed strong reactivity of the newly deposited dentin matrix (Figure 7 I), a confirmation that the newly formed dentin matrix was of human origin (new human dentin deposited by HODCs) and not mouse cells. Similarly, the anti-human DMP1 did not react with mouse dentin (Figure 7J) to further confirm that the newly deposited dentin was human dentin deposited by HODCs and not mouse cells.

Newly formed HODC-induced predentin displayed distinct dentinal tubules (Figure 8A) suggestive of trans-differentiation of HODCs to dentin-secreting odontoblasts. There was a clear interface between proliferating HODCs and newly deposited predentin. This transition zone contained a composite of cells and dentin matrix that confirms that HODCs participated in deposition of the new dentin matrix (Figure 8B). Interestingly, an island of predentin with a central core of fibroblast-like cells, blood vessel and hematopoietic tissues appeared to mimic the cross-section of a root canal with pulp tissue (Figure 8 C and D). These predentin islands were absent in DPSC and BMSC transplants.

Discussion

All the odontomas were characteristically similar based on the haphazard spatial arrangements of enamel, dentin, cementum and an abundance of cells. The native cells within the odontoma expressed high levels of Wnt-1 and β -catenin that have been implicated in tooth development and formation of supernumerary teeth (Liu et al., 2007). This may relate to earlier report that mice engineered to constitutively express stabilized β -catenin display continuous tooth regeneration (Jarvinen et al., 2006). While Wnt/ β -catenin signaling is active at multiple stages of tooth development (Liu et al., 2007) and β -catenin has been demonstrated in odontogenic epithelium of odontoma (Tanaka et al., 2007), the location of Wnt-1 and β -catenin in the complex odontoma may not necessary indicate active canonical Wnt signaling. Further characterization of the odontoma cellular contents was enhanced by isolating HODCs from a complex odontoma obtained from one female patient using previously developed methodology. Similar to previously described DPSCs (Gronthos et al., 2000), HODCs

displayed multipotent stem cell properties. But the higher expression of both early (nestin, Sox-2) and late (β III-tubulin) neural stem cell markers as well as DMP-1 (a dental marker) suggest a potential ability of HODCs to form multiple tissues more readily than DPSCs. Without using neural induction supplements in the culture medium, several single clones readily changed morphology to display stretched-out dendrite-like cytoplasmic projections.

The ease of HODC neural differentiation without additional induction suggests that HODCs may be rich in neural progenitor cells. It is also possible that continual renewal of dental tissues such as secondary and tertiary dentin by resident progenitor cells is necessary to maintain dental pulp integrity and health. The proliferative and survival capacities of HODCs compared favorably well with DPSCs as they demonstrated a ‘catch-up’ proliferation when given more time to grow. This is noteworthy because *ex vivo* expansion will be necessary to obtain large quantities of HODCs if it will serve as a viable donor graft material for dental tissue regeneration. Combination of hydroxyapatite and tricalcium phosphate (HA/TCP) served as a good inducer of trans-differentiation because HODCs attached to HA/TCP to form hard tissues resembling cementum or possibly bone just like those formed by BMSCs. The hard tissues regenerated by DPSCs-HA/TCP complex were less cellular resembling more of acellular cementum rather than bone. The dentin shell and PCL served as good inducers of dentinogenesis because new predentin was deposited in a linear fashion along the dentin shell with entrapped HODCs within the predentin matrix. Since epithelial-mesenchymal interactions are necessary to form a complete tooth, it was not unusual that HODCs cells did not form enamel when transplanted with either HA/TCP or PCL. Further work is still warranted on interaction of HODCs with epithelial cells and the possibility of regenerating all the essential components of a human tooth. HODCs represent a unique post-natal stem cell population that readily differentiate to neural cells and commit to the formation of more than one type of dental tissue. They share multipotent properties with DPSCs and BMSCs but have more superior dental regenerative properties than both cell types. Given the right induction, HODCs can form nerve cells, dentin and cementum making it a good donor tissue for dental repair and regeneration.

Acknowledgments

The authors express gratitude to Dr. Larry Fisher (National Institute of Dental and Craniofacial Research/National Institutes of Health (NIDCR/NIH), Bethesda, MD) for the gift of monoclonal antibody to human DMP1 (LFMb-31), Zimmer Inc, Warsaw, IN for the gift of hydroxyapatite/tricalcium phosphate and Solvay Caprolactones, Houston TX for the gift of polycaprolactone. We also acknowledge the support of Drs. Michael Collins and Pamela Gehron Robey (NIDCR/NIH) at the early stages of this project and the useful comments of Drs. Carolyn Gibson (University of Pennsylvania, Philadelphia PA) Ho-Keel Hwang (Chosun University, Gwangju, Korea) and Eui-Seong Kim (Yonsei University, Seoul, Korea). This project was partly funded by USPHS research grant 5K08CA120875-02 from the National Cancer Institute/NIH, Bethesda, MD 20892.

References

- Akintoye SO, Lam T, Shi S, Brahim J, Collins MT, Robey PG. Skeletal site-specific characterization of orofacial and iliac crest human bone marrow stromal cells in same individuals. *Bone* 2006;38:758–768. [PubMed: 16403496]
- el-Saggan A, Bang G, Olofsson J. Melanotic neuroectodermal tumour of infancy arising in the maxilla. *J Laryngol Otol* 1998;112:61–64. [PubMed: 9538448]
- Ernst LM, Quinn PD, Alawi F. Novel oral findings in Schimmelpenning syndrome. *Am J Med Genet A* 2007;143:881–883. [PubMed: 17366580]
- Garcia-Castro MI, Marcelle C, Bronner-Fraser M. Ectodermal Wnt function as a neural crest inducer. *Science* 2002;297:848–851. [PubMed: 12161657]
- Graham V, Khudyakov J, Ellis P, Pevny L. SOX2 functions to maintain neural progenitor identity. *Neuron* 2003;39:749–765. [PubMed: 12948443]

- Gronthos S, Mankani M, Brahimi J, Robey PG, Shi S. Postnatal human dental pulp stem cells (DPSCs) in vitro and in vivo. *Proc Natl Acad Sci U S A* 2000;97:13625–13630. [PubMed: 11087820]
- Grzesik WJ, Kuznetsov SA, Uzawa K, Mankani M, Robey PG, Yamauchi M. Normal human cementum-derived cells: isolation, clonal expansion, and in vitro and in vivo characterization. *J Bone Miner Res* 1998;13:1547–1554. [PubMed: 9783543]
- Jarvinen E, Salazar-Ciudad I, Birchmeier W, Taketo MM, Jernvall J, Thesleff I. Continuous tooth generation in mouse is induced by activated epithelial Wnt/beta-catenin signaling. *Proc Natl Acad Sci U S A* 2006;103:18627–18632. [PubMed: 17121988]
- Kuznetsov SA, Krebsbach PH, Satomura K, Kerr J, Riminucci M, Benayahu D, Robey PG. Single-colony derived strains of human marrow stromal fibroblasts form bone after transplantation in vivo. *J Bone Miner Res* 1997;12:1335–1347. [PubMed: 9286749]
- Lendahl U, Zimmerman LB, McKay RD. CNS stem cells express a new class of intermediate filament protein. *Cell* 1990;60:585–595. [PubMed: 1689217]
- Liu F, Chu EY, Watt B, Zhang Y, Gallant NM, Andl T, Yang SH, Lu MM, Piccolo S, Schmidt-Ullrich R, Taketo MM, Morrisey EE, Atit R, Dlugosz AA, Millar SE. Wnt/beta-catenin signaling directs multiple stages of tooth morphogenesis. *Dev Biol*. 2007
- Mankani MH, Kuznetsov SA, Fowler B, Kingman A, Robey PG. In vivo bone formation by human bone marrow stromal cells: effect of carrier particle size and shape. *Biotechnol Bioeng* 2001;72:96–107. [PubMed: 11084599]
- Miura M, Gronthos S, Zhao M, Lu B, Fisher LW, Robey PG, Shi S. SHED: stem cells from human exfoliated deciduous teeth. *Proc Natl Acad Sci U S A* 2003;100:5807–5812. [PubMed: 12716973]
- Ogbureke KU, Fisher LW. Expression of SIBLINGs and their partner MMPs in salivary glands. *J Dent Res* 2004;83:664–670. [PubMed: 15329369]
- Osydzka AM, Diefenderfer DL, Bhargava G, Leboy PS. Different effects of BMP-2 on marrow stromal cells from human and rat bone. *Cells Tissues Organs* 2004;176:109–119. [PubMed: 14745240]
- Robey PG. Collagenase-treated trabecular bone fragments: a reproducible source of cells in the osteoblastic lineage. *Calcif Tissue Int* 1995;56 Suppl 1:S11–S12. [PubMed: 7719973]
- Sapp JP, Eversole LR, Wysocki GP. Contemporary oral and maxillofacial pathology. Mosby, St. Louis, Mo. 2004
- Seo BM, Miura M, Gronthos S, Bartold PM, Batouli S, Brahimi J, Young M, Robey PG, Wang CY, Shi S. Investigation of multipotent postnatal stem cells from human periodontal ligament. *Lancet* 2004;364:149–155. [PubMed: 15246727]
- Sharpe PT. Neural crest and tooth morphogenesis. *Adv Dent Res* 2001;15:4–7. [PubMed: 12640730]
- Slavkin HC, MacDougall M, Zeichner-David M, Oliver P, Nakamura M, Snead ML. Molecular determinants of cranial neural crest-derived odontogenic ectomesenchyme during dentinogenesis. *Am J Med Genet* 1988 Suppl 4:7–22.
- Sonoyama W, Liu Y, Fang D, Yamaza T, Seo BM, Zhang C, Liu H, Gronthos S, Wang CY, Shi S, Wang S. Mesenchymal stem cell-mediated functional tooth regeneration in swine. *PLoS ONE* 2006;1:e79. [PubMed: 17183711]
- Sonoyama W, Seo BM, Yamaza T, Shi S. Human Hertwig's epithelial root sheath cells play crucial roles in cementum formation. *J Dent Res* 2007;86:594–599. [PubMed: 17586703]
- Stefanik D, Sarin J, Lam T, Levin L, Leboy PS, Akintoye SO. Disparate osteogenic response of mandible and iliac crest bone marrow stromal cells to pamidronate. *Oral Dis* 2008;14:465–471. [PubMed: 18938273]
- Tanaka A, Okamoto M, Yoshizawa D, Ito S, Alva PG, Ide F, Kusama K. Presence of ghost cells and the Wnt signaling pathway in odontomas. *J Oral Pathol Med* 2007;36:400–404. [PubMed: 17617832]
- Thesleff I, Hurmerinta K. Tissue interactions in tooth development. *Differentiation* 1981;18:75–88. [PubMed: 7011890]
- Thesleff I, Partanen AM, Vainio S. Epithelial-mesenchymal interactions in tooth morphogenesis: the roles of extracellular matrix, growth factors, and cell surface receptors. *J Craniofac Genet Dev Biol* 1991;11:229–237. [PubMed: 1725871]
- Thesleff I, Vaahtokari A, Partanen AM. Regulation of organogenesis. Common molecular mechanisms regulating the development of teeth and other organs. *Int J Dev Biol* 1995;39:35–50. [PubMed: 7626420]

Yamashiro T, Zheng L, Shitaku Y, Saito M, Tsubakimoto T, Takada K, Takano-Yamamoto T, Thesleff I. Wnt10a regulates dentin sialophosphoprotein mRNA expression and possibly links odontoblast differentiation and tooth morphogenesis. *Differentiation* 2007;75:452–462. [PubMed: 17286598]

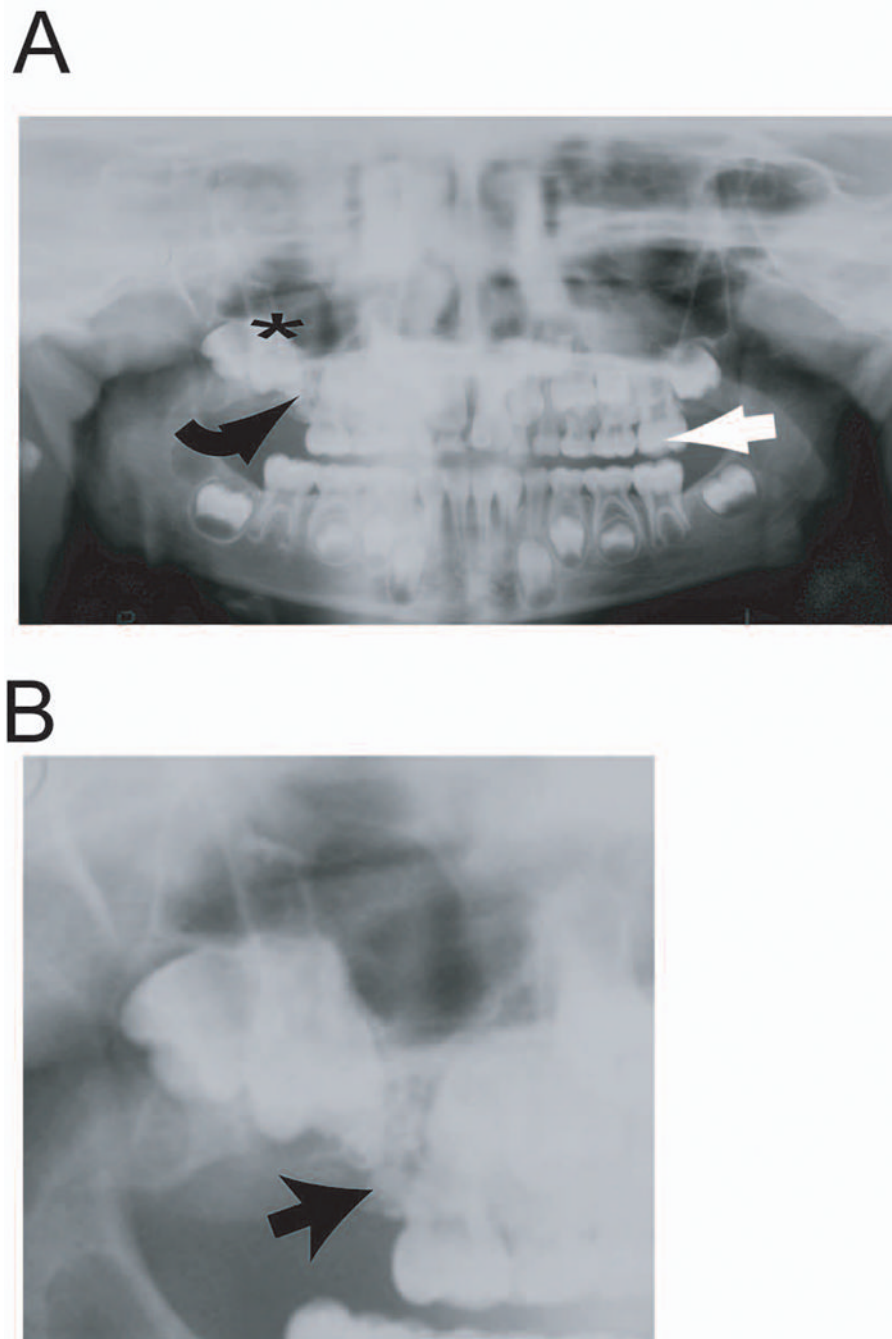


Figure 1. Representative panoramic radiograph demonstrating location of odontoma. A complex odontoma is present in the right maxilla of this 7 year-old female patient (A). The location of the odontoma (curved black arrow) blocked eruption of the fully-developed right maxillary first molar (black star). Note the left maxillary first molar (straight white arrow) is fully erupted and in occlusion with the opposing mandibular first molar. More detailed evaluation of odontoma (B) shows there are multiple odontomas blocking normal eruption pattern of the permanent maxillary molar.

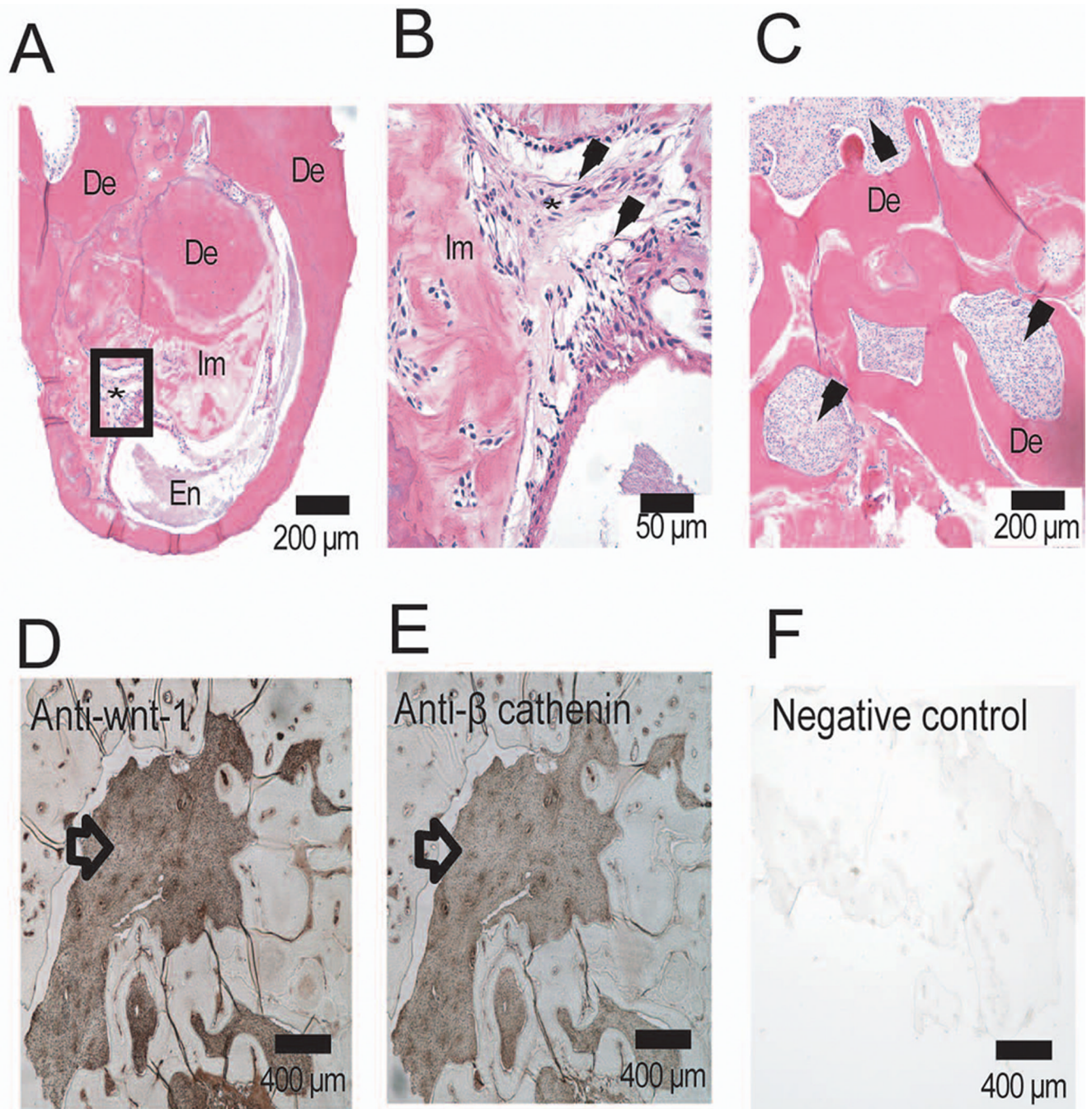


Figure 2. Cellular components of odontoma. Hematoxylin-eosin-stained section of odontoma (A) showing outer layer of dentin (De) surrounding inner layers of enamel (En), immature matrix (Im) and a rich cellular components (*). Higher magnification of cellular components in A (box) is presented in B. This shows heterogeneous staining fibroblast-like cells (arrows) mixed with immature matrix at different stages of mineralization (B). Another section of the odontoma showed compartmentalization of the cellular fibroblastic network by dentin-like matrix (C). Odontoma cellular contents immunoreacted positively with goat polyclonal antibody to human Wnt1-1 (D) and mouse monoclonal antibody to human β -catenin (E). Non-immune goat serum (F) and IgG isotype control were unreactive.

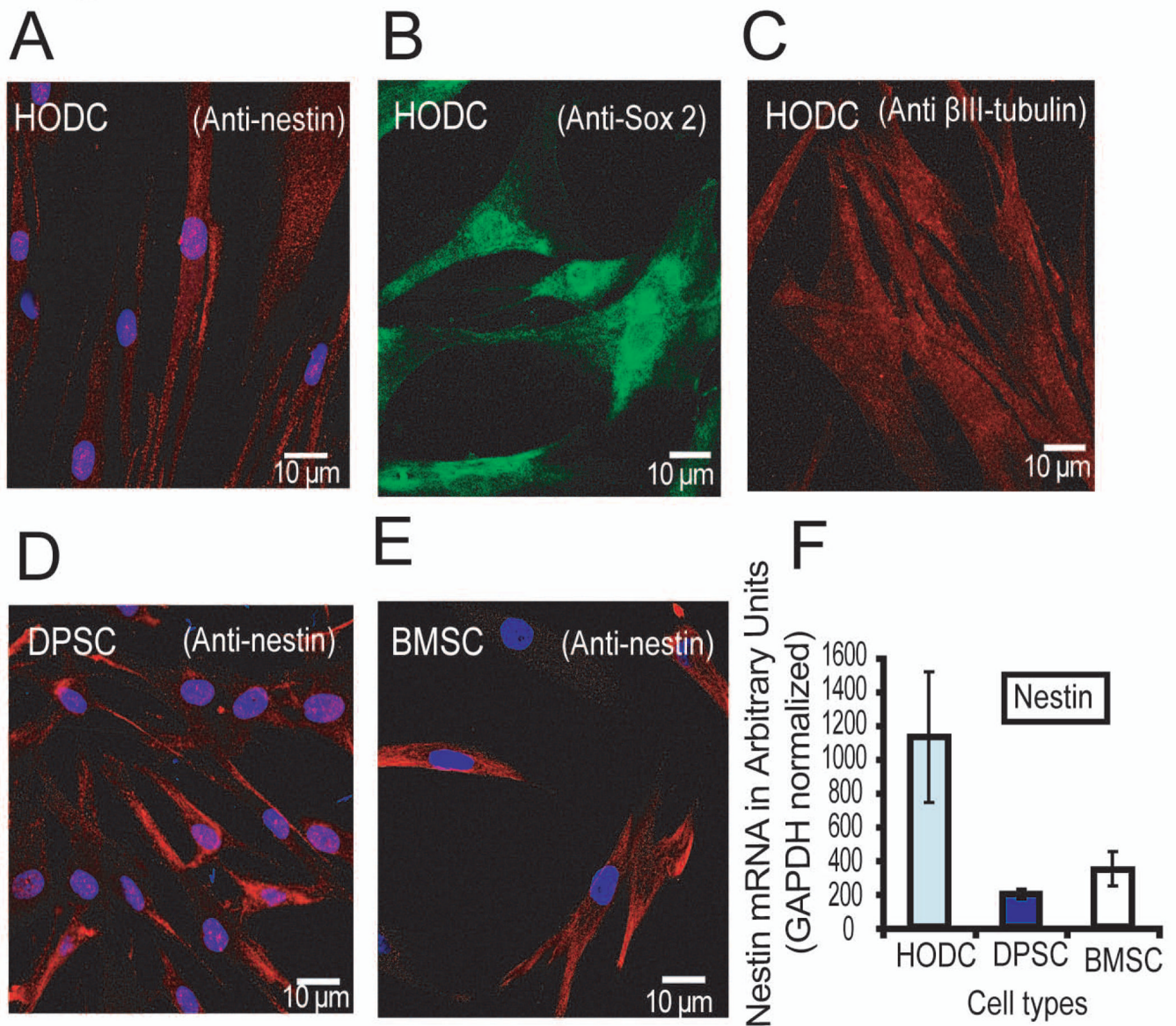


Figure 3. Immunoreactivity of HODCs with neural markers. Early passage (passages 2 and 3) HODCs immunoreacted positively with markers of early neural stem cell progenitors that included nestin (A) and Sox-2 (B), and a late marker of neural differentiation, βIII-tubulin. Comparatively, both DPSCs and maxilla BMSCs only immunoreacted with nestin (D and E respectively). Quantitative analysis by real time-PCR showed a significantly much higher nestin expression ($P < 0.04$) by HODCs than either DPSCs or maxilla BMSCs (F). There was no statistically significant differences between DPSCs and BMSCs. Primary anti-human Sox-2 was labeled with AlexaFluor 488 goat-anti-mouse secondary antibody while primary anti-human nestin and anti-human βIII-tubulin were labeled with AlexaFluor 555 goat anti-mouse secondary antibody. [GAPDH = glyceraldehyde-3-phosphate dehydrogenase].

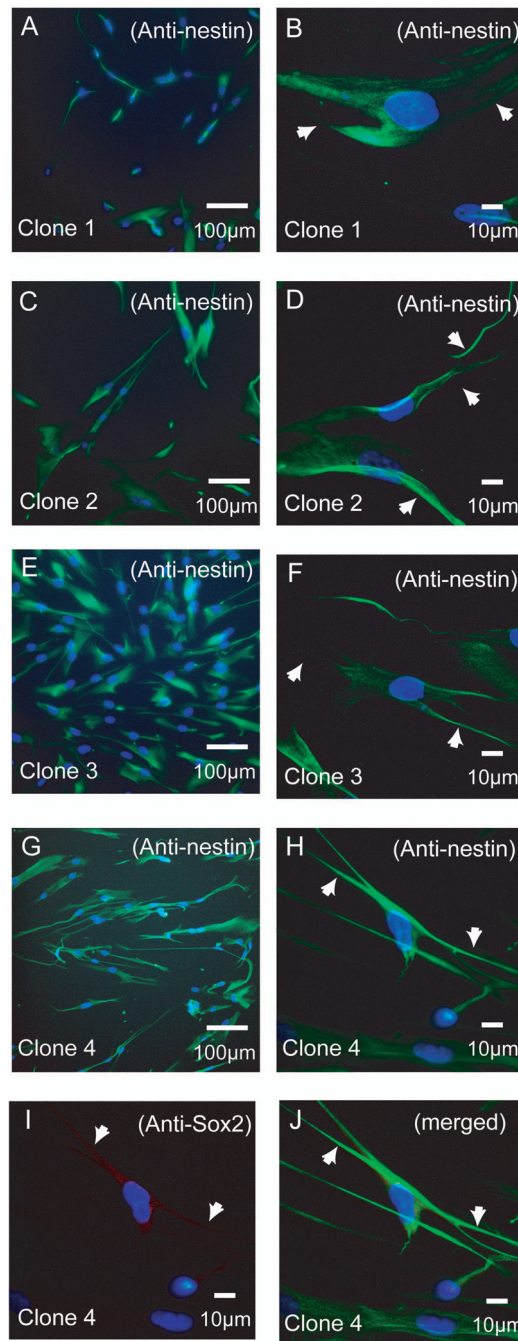


Figure 4. Immunophenotype of single colony-derived strains of HODCs. All the four clones tested reacted strongly with nestin (A–H). They acquired narrow stretched-out dendrite-like cytoplasmic projections (white arrows) resembling neural cells (B, D, F, H, I and J). Single clones were also immunoreactive with Sox 2 as shown by a representative sample (I). Sox 2 did not co-localized with nestin (J).

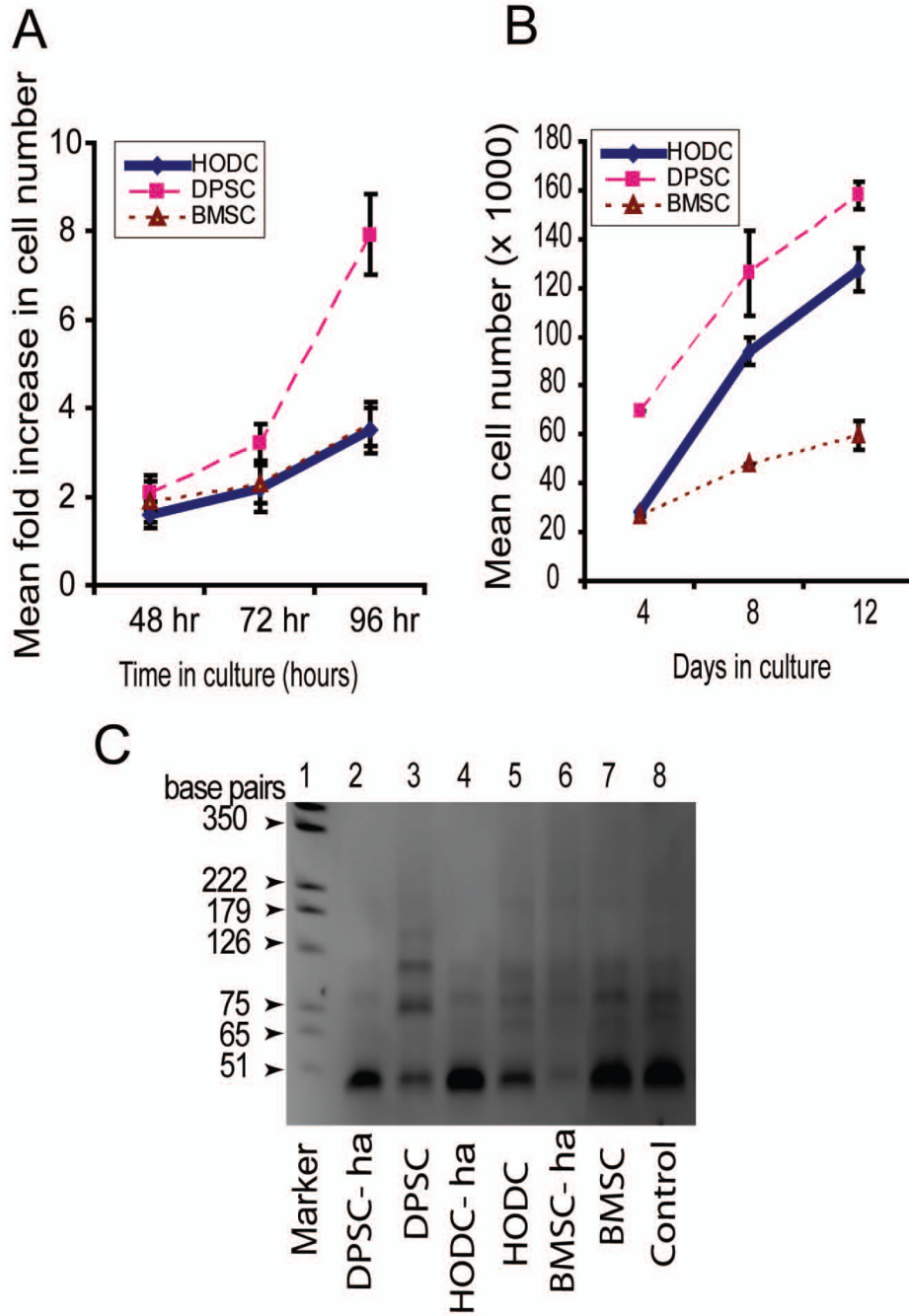


Figure 5. Proliferative and survival capacities of HODCs. Early passage (passages 2 and 3) HODCs were less proliferative compared with DPSCs but demonstrated similar proliferative capacity with mandible BMSCs during 96 hours of culture. Prolonged culture for 12 days showed a dramatic increase in survival capacity of HODCs compared with mandible BMSCs that was still less than that of DPSCs (B). Step-ladder pattern of a TRAPEze assay (C) showed corresponding higher level of human telomerase in DPSCs (lane 3) while HODCs (lane 5) and BMSCs (lane 7) were lower but similar. [ha = heat inactivated control; lane 8 = telomerase positive control].

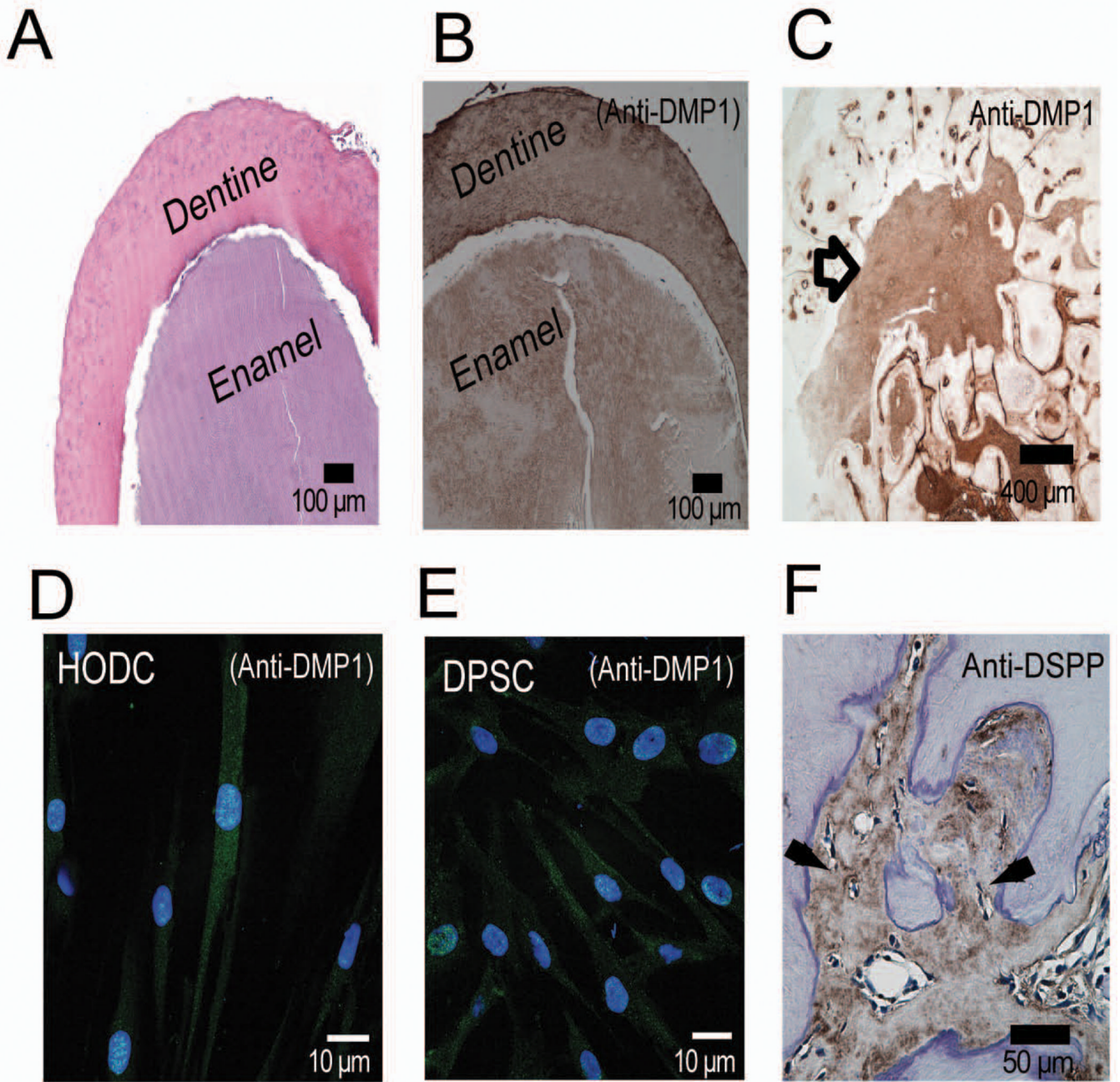


Figure 6. Expression of dentin-related markers by odontoma and HODCs. Hematoxylin and eosin-stained section of odontoma showed distinct reversal of enamel and dentin spatial relationship. The more centrally located enamel is surrounded by an outer dentin layer (A). Both enamel and dentin immunostained positively with anti-DMP1 (B), an indication of mixed cell populations differentiating to dental hard tissues. The cellular contents of odontoma (C) and HODCs (D) immunoreacted strongly with anti-DMP1. Cell contents of odontoma tissue and HODCs both immunoreacted strongly with DMP1 just like DPSCs (E). The cellular contents of odontoma were positive for DSPP but the matrix was unreactive (F). Primary anti-human DMP1 was labeled with AlexaFluor 488 goat anti-mouse secondary antibody.

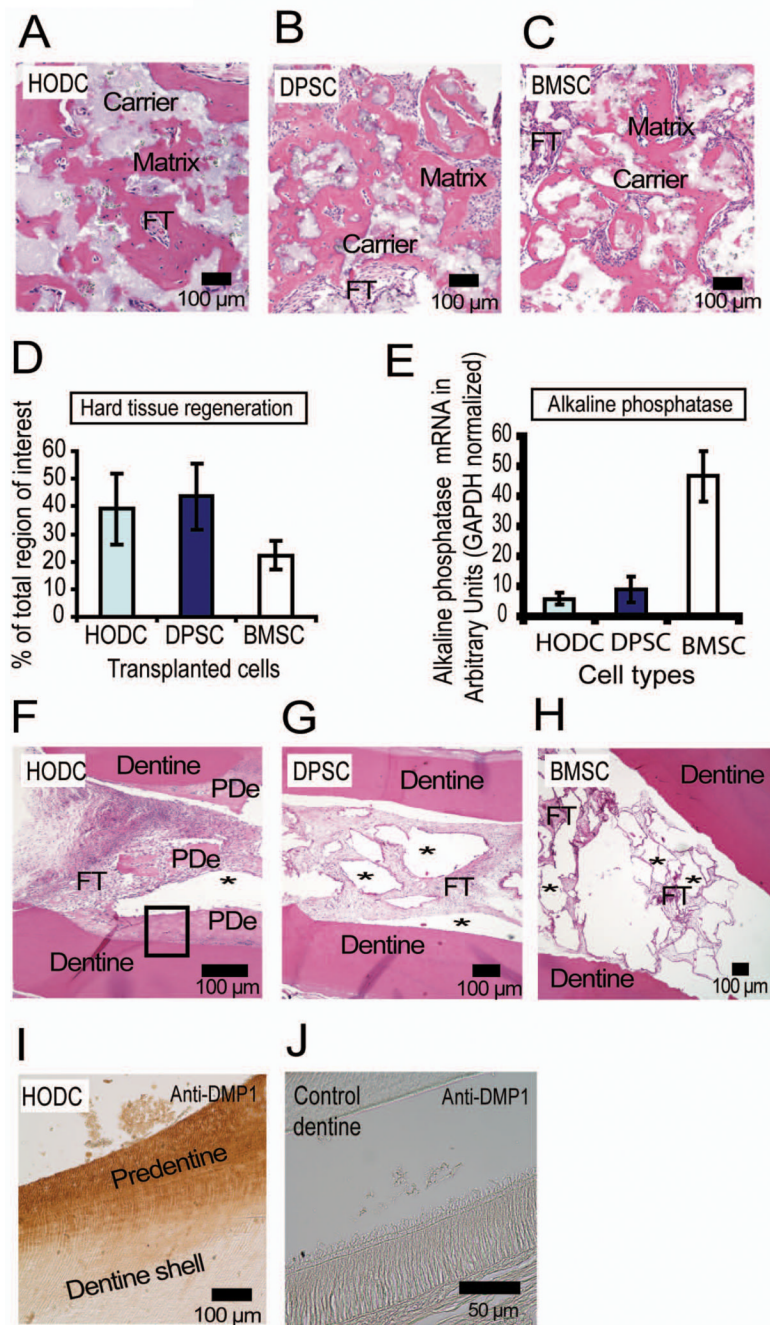


Figure 7.

Hard tissue regenerative capacity of transplanted HODCs. Transplantation of HODCs and control cells (DPSC and BMSC) into immunocompromised mice with hydroxyapatite/tricalcium phosphate (HA/TCP) as ceramic carrier regenerated hard tissues that resembled either cementum or bone (A, B and C). Note more cells trapped in the matrix formed by HODC (A) and BMSC (C) compared with DPSC (B). Analysis of the hard tissues showed that HODCs and DPSCs formed more hard tissues than BMSCs (D) but the cells' ability to express alkaline phosphatase assessed by real-time PCR was highest in BMSCs ($P < 0.001$, E). Cell transplantation with polycaprolactone as carrier within a dentin shell induced formation of predentin (PDe) in HODCs transplants (F) while DPSCs and BMSCs did not regenerate any hard tissues (G and

H). Note the clear empty regions (*) previously occupied by resorbed polycaprolactone. Newly formed predentin (F, box) reacted strongly with anti-human DMP1 which confirmed human origin of new predentin (I). [FT = fibrous tissue].

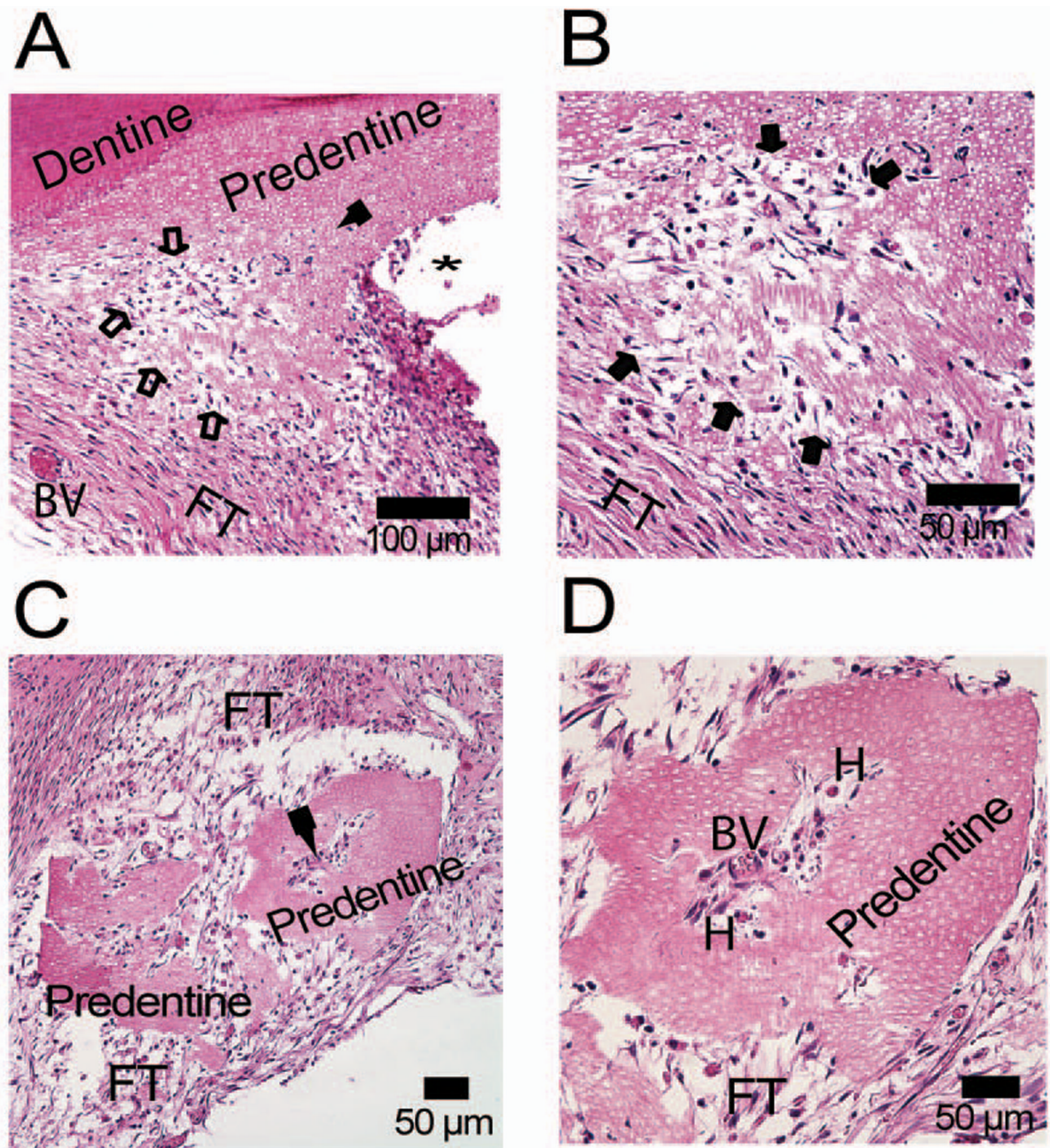


Figure 8. Regeneration of predentin by HODCs. Predentin deposited by HODCs on dentin shell is demonstrated by a distinct transition zone between dentin and predentin (A). Note the characteristic patchy clear zones in the predentin representing odontoblastic processes (solid arrow) and the advancing edge of new predentin deposition (open arrows). Higher magnification showed clearly the advancing predentin margin (solid arrows) and odontoblastic processes (B). A circumscribed section of predentin is shown enclosing tissue elements (solid arrow) that resemble dental pulp (C). Higher magnification of the pulp-like region showed blood vessel (BV) containing erythrocytes and amorphous hematopoietic materials (H). DPSCs and BMSCs did not regenerate any such hard tissues as shown in Figure 7. [FT = fibrous tissue].

Table 1

Patient demography, location and histological characteristics of odontomas

| Patient # | Age (years) | Sex | Jaw location | Histological variety |
|-----------|-------------|-----|--------------|----------------------|
| 1 | 6 | F | Maxilla | Complex |
| 2 | 6 | F | Mandible* | Complex |
| 3 | 7 | F | Maxilla | Complex |
| 4 | 9 | M | Maxilla * | Compound |
| 5 | 10 | F | Maxilla | Complex |
| 6 | 11 | M | Maxilla | Compound |
| 7 | 16 | M | Mandible | Compound |
| 8 | 19 | F | Maxilla | Complex |
| 9 | 21 | F | Mandible | Complex |
| 10 | 25 | M | Mandible | Complex |
| 11 | 25 | F | Mandible | Compound |
| 12 | 27 | F | Mandible | Complex |
| 13 | 35 | F | Maxilla | Compound |
| 14 | 49 | M | Mandible | Complex |

M = male; F = female;

* = anterior jaw